International Multidisciplinary Journal of Emerging Technologies and Applications (IMJETA)
Vol. 1, No. 1, pp. 1-17, April 2026
Received April 09, 2026; Revised April 12, 2026; Accepted April 22, 2026
Published April 30, 2026

A Comparative Analysis of Convolutional Neural Networks for Automated Myopia Classification via Fundus Imaging

Danny Noe Cuaquira Huachaca[1][0009-0009-0717-6766] and Manuel J. Ibarra-Cabrera[2][0000-0001-6711-4916]

[1]Escuela Profesional de Ingeniería Informática y Sistemas, Universidad Nacional Micaela Bastidas de Apurímac, Abancay, Peru
192193@unamba.edu.pe

[2]Departamento Académico de Informática y Sistemas, Universidad Nacional Micaela Bastidas de Apurímac, Abancay, Peru
mibarra@unamba.edu.pe

Abstract. According to recent reports from the World Health Organization (WHO), myopia now affects 30% of the global population and continues to rise steadily. Given that early detection is critical for timely and effective treatment. This study evaluates and compares the performance of two prominent convolutional neural network (CNN) architectures—ResNet50 and InceptionV3—for the automated classification of myopia using blue-light fundus imagery. Employing a cross-sectional, non-experimental design, the research utilized a large-scale dataset of 124,794 images (63,294 Myopia; 61,500 Normal). The data were partitioned into training (70%), validation (20%), and testing (10%) sets. Models were implemented in Python using TensorFlow and Keras, leveraging the Google Colab Pro environment with A100 GPU acceleration. To mitigate overfitting and enhance generalization, rigorous preprocessing and data augmentation techniques were applied. Experimental results indicate that both architectures achieved exceptional performance; notably, InceptionV3 outperformed ResNet50, achieving a validation accuracy of 99.97% and a significantly lower loss of 0.0075. These results confirm the robustness of deep learning models for clinical myopia screening in response to the growing global prevalence.

Keywords: Myopia; Convolutional Neural Network; Fundus Imagery; Deep Learning.

1. Introduction

Myopia represents a leading cause of global visual impairment and blindness (Steinmetz et al., 2021), with its prevalence rising at an alarming rate (Fricke et al., 2018). The World Health Organization (WHO) estimated that over 2.5 billion individuals were affected by myopia in 2020; projections suggest this figure could escalate to 5 billion by 2050 in the absence of effective interventions (Singh et al., 2022). This trend is acutely evident in rapidly urbanizing regions of East Asia,

including Japan, South Korea, and China, where over 80% of adolescents are myopic and approximately 10% have developed high myopia (Holden et al., 2016). While the condition typically manifests during childhood and stabilizes in late adolescence (Primadiani & Rahmi, 2017), its progression is influenced by a combination of genetic factors (Laksono & Winarno, 2025) and environmental stressors, such as inadequate lighting, near-work habits, and the excessive use of electronic devices (Zahra et al., 2024; Puspitasari et al., n.d.).

The WHO advocates for routine ocular examinations as a primary strategy for early detection (Simarmata et al., 2024). However, conventional refractive procedures often require specialized equipment and in-person clinical expertise, significantly limiting accessibility in underserved regions. Consequently, uncorrected refractive errors remain a primary driver of visual impairment worldwide (Sambulele et al., 2025). Within this landscape, digital fundus imaging has emerged as a transformative diagnostic tool. By providing detailed visualizations of the retina, fundus photographs offer essential data for monitoring eye health and identifying complications associated with high myopia, which can lead to irreversible vision loss if not addressed through timely intervention (Primadiani & Rahmi, 2017).

Recent technological advances have shifted focus toward Artificial Intelligence (AI) for the automated analysis of fundus images. Deep learning, a subset of machine learning utilizing multi-layered neural networks, enables the processing of vast datasets with high computational efficiency (Hartati, 2024). Convolutional Neural Networks (CNNs) have proven particularly effective in this domain due to their inherent ability to autonomously learn hierarchical spatial features and maintain invariance to image transformations such as scaling and rotation (Wardhani et al., 2024). While previous research has explored texture analysis (Cahya et al., 2021) and hybrid models like CNN-KNN for general ocular diseases, there remains a critical need for focused comparative studies on specific CNN architectures optimized for myopia classification.

This study aims to address the following research question: Which convolutional neural network architecture—InceptionV3 or ResNet50—demonstrates superior performance in classifying myopia within fundus images? Performance is evaluated across multiple metrics, including precision, accuracy, recall, loss, and F1-score. Utilizing a large-scale retinal dataset, the models were implemented in a reproducible Python environment using Keras and TensorFlow. To ensure high-performance computing, training was conducted via Google Colab Pro, leveraging NVIDIA A100 GPUs with high RAM capacity.

The primary contribution of this research is the provision of empirical evidence regarding the comparative effectiveness and feasibility of these architectures for myopia diagnosis. Furthermore, this study advocates for the development of affordable, AI-driven diagnostic solutions suitable for rural or resource-limited areas. Ultimately, the methodology presented herein serves as a framework that can

be extended to the detection of other refractive errors, such as astigmatism and hyperopia, fostering broader visual health equity.

Similarly, it can be said that this work, this research on automated myopia classification via CNNs directly supports the United Nations' Sustainable Development Goals (SDGs) (United Nations, n.d.) by enhancing global healthcare accessibility. By leveraging AI for early detection, it advances SDG 3 (Good Health and Well-being) through the prevention of avoidable blindness and SDG 4 (Quality Education) by ensuring vision impairment does not hinder student learning. Furthermore, it fosters SDG 9 (Industry, Innovation, and Infrastructure) by integrating cutting-edge technology into public health and promotes SDG 10 (Reduced Inequalities) by providing high-quality diagnostic tools.

2. Related Work

Artificial intelligence (AI) has become a cornerstone of ocular disease screening in recent years (Sait & Rahaman, 2023). Recent benchmarks underscore the efficacy of these technologies; for instance, a study utilizing the EfficientNetB0 architecture achieved 97% accuracy in differentiating myopic from non-myopic fundus images (Laksono & Winarno, 2025). This research, which utilized the same 'Myopia Image Dataset' employed in the present study, further validates the capacity of Convolutional Neural Networks (CNNs) for automated myopia detection.

Beyond myopia, the versatility of deep learning architectures has been demonstrated across various ophthalmic conditions. In 2022, the Inception-v3 model reached an accuracy of 98.52% in classifying glaucoma using the ACRIMA dataset, highlighting its reliability as a clinical diagnostic aid (Shyamalee & Meedeniya, 2022). Furthermore, specialized architectures have been developed to address pathological myopia and its complications. For example, Swain and R. (2023) implemented a hybrid U-Net and CNN framework that attained a classification accuracy of 97.8%.

Continued advancements in 2025 have further refined these capabilities. Kaya (2025) utilized a combined U-Net and ResNet model to segment optic atrophy and the optic disc, achieving 96.7% accuracy in pathological myopia segmentation. Similarly, Zhang et al. (2025) enhanced the detection of myopic maculopathy through a self-supervised learning architecture, achieving 96.8% accuracy on internal datasets. While these studies demonstrate high performance, the performance drop observed by Zhang et al. on external datasets (89.0%) emphasizes the ongoing challenge of model generalization across diverse imaging environments.

3. Methodology

3.1 Type and Level

This research is categorized as applied study, as it prioritizes the implementation and evaluation of Convolutional Neural Network (CNN) architectures to address a

critical diagnostic challenge in ocular health: the automated detection of myopia via fundus imaging.

The study employs a descriptive-comparative design, systematically analyzing the performance of the ResNet50 and InceptionV3 architectures. Rather than seeking to establish new theoretical frameworks, the objective was to conduct a rigorous benchmarking of these models using a standardized dataset. Performance was quantified through established performance metrics, including precision, recall, accuracy, F1-score, and categorical cross-entropy loss, to determine the most effective architecture for distinguishing myopic conditions from healthy ocular states.

3.2 Research Design

The study employed a cross-sectional, non-experimental design, utilizing a pre-existing dataset without modifying the underlying data structures. Two prominent convolutional neural network (CNN) architectures—ResNet50 and InceptionV3—were implemented to perform binary classification on fundus imagery, distinguishing between myopic and normal ocular states.

3.3 Participants

The study utilized a substantial dataset of 124,794 fundus images, characterized by a balanced distribution between myopic (n = 63,294) and normal (n = 61,500) cases. These images were sourced from established public repositories frequently utilized in the literature, specifically the Myopia Image Dataset hosted on Kaggle. Table 1 details de dataset.

Table 1: Source and details of the dataset

Dataset	
Description	Myopia Image Dataset
Amount of data	124.749 images
Tags	Myopia, Normal
URL	https://www.kaggle.com/datasets/kellysanderson/myopia-image-dataset

During the experimental phase, the dataset was partitioned into three subsets: 70% for training, 20% for validation, and 10% for testing. This distribution was automated via a custom Python script to ensure consistency. To mitigate selection bias and ensure a balanced class representation across all subsets, the process utilized stochastic shuffling and stratified folder allocation. The implementation leveraged standard libraries, including “shutil, os”, and “random”, ensuring a reliable and reproducible data pipeline for subsequent model evaluation.

Table 2 details the configuration parameters for data preprocessing and model training. Data augmentation techniques were applied exclusively during the training phase to enhance the models' generalization capability and serve as a

regularization strategy to mitigate overfitting. Conversely, the validation and test sets were processed using only the standard baseline preprocessing required by each respective architecture.

Table 2: Preprocessing configuration and model training

Feature	InceptionV3	ResNet50
Model type	Pre-trained CNN	Pre-trained CNN
Methodology	Transfer learning	Transfer learning
Input size	224 × 224 × 3 (RGB)	224 × 224 × 3 (RGB)
Preprocessing	preprocess_input (InceptionV3)	preprocess_input (ResNet50)
Data augmentation (training)	Rotation, zoom, horizontal flip	Rotation, shift, horizontal flip
Data augmentation (validation/testing)	Not applied	Not applied
Objective	Binary classification (Myopia vs. Normal)	Binary classification (Myopia vs. Normal)

The retinal imagery utilized in this research is illustrated in Figures 1 and 2, while the architectural frameworks for ResNet50 and InceptionV3 are presented in Figures 3 and 4, respectively. The fundus image in Figure 1, obtained from the 'Myopia Image Dataset', displays distinct morphological alterations characteristic of myopia. Specifically, it reveals axial elongation and structural shifts in the fundus—findings that align with established anatomical literature regarding the progression of axial myopia (Jonas et al., 2023).

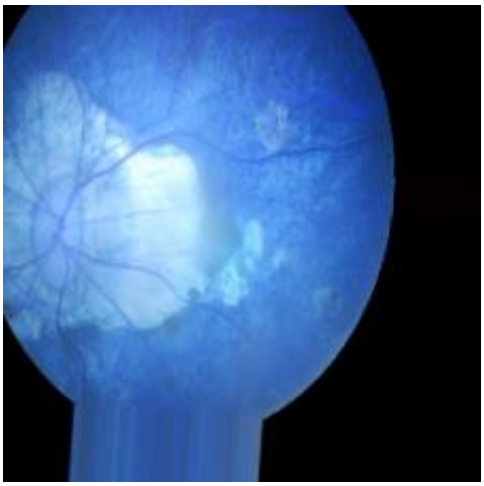

Figure 1. Image of a retina with myopia

The image presented in Figure 2 represents a healthy retina and was sourced from the 'Myopia Image Dataset.' It serves as a baseline for a healthy, emmetropic eye, where no clinical signs of myopia are present in the fundus. In such cases, the retina

is free from common abnormalities such as choroidal thinning, posterior staphyloma, optic nerve distortion, or chorioretinal atrophy. The absence of these morphological markers distinguishes a healthy state from the degenerative changes observed in high myopia; previous studies have confirmed that these specific anomalies are highly correlated with axial elongation and the long-term progression of the condition (Jonas et al., 2023).

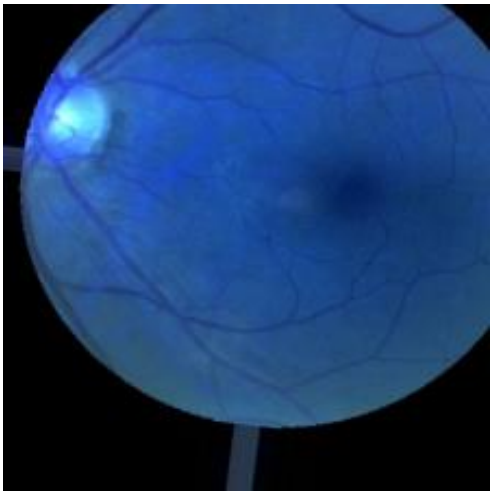

Figure 2. Image of a normal retina

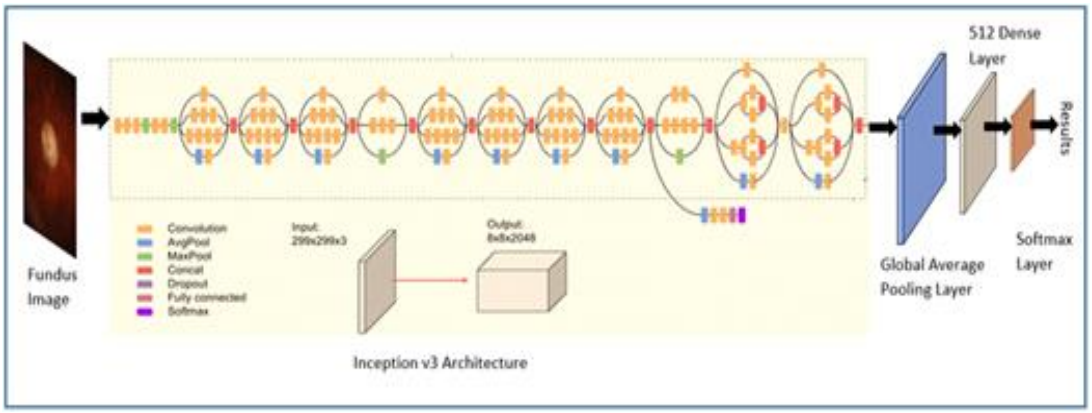

Figure 3. InceptionV3 Architecture

Inception-v3, introduced by Google in 2015, represents a landmark convolutional neural network (CNN) architecture optimized for advanced visual recognition tasks. Its core innovation lies in the use of Inception modules, which employ factorized convolutions and dimension reduction to enhance computational efficiency without sacrificing depth. Benchmarks on the ImageNet dataset have demonstrated its robustness, achieving a top-1 accuracy of approximately 78.1% and a top-5 accuracy exceeding 93.9% (Szegedy et al., 2016). The specific architectural modifications implemented for this myopia classification study are illustrated in Figure 3.

ResNet50 is a residual deep convolutional neural network consisting of 50 layers, specifically engineered to mitigate the vanishing gradient problem through the implementation of skip connections or residual blocks (He et al., 2016). Computationally, the architecture requires approximately 3.8×10^9 floating-point operations (FLOPs) and comprises 48 convolutional layers alongside specialized Max Pooling and Average Pooling layers. In this research, we utilized a pre-trained version of ResNet50, originally optimized on more than one million images from the ImageNet dataset (Celano, 2021).A fine-tuning strategy was adopted to repurpose the model for the binary classification of fundus imagery (Myopia vs. Normal). This adaptation involved the removal of the original top-level fully connected layers, which were replaced with a new classification head consisting of a 256-neuron dense layer utilizing the ReLU activation function. Finally, a single-neuron output layer with a Sigmoid activation was integrated to generate the probability distribution for the myopia class. The resulting modified architecture is detailed in Figure 4.

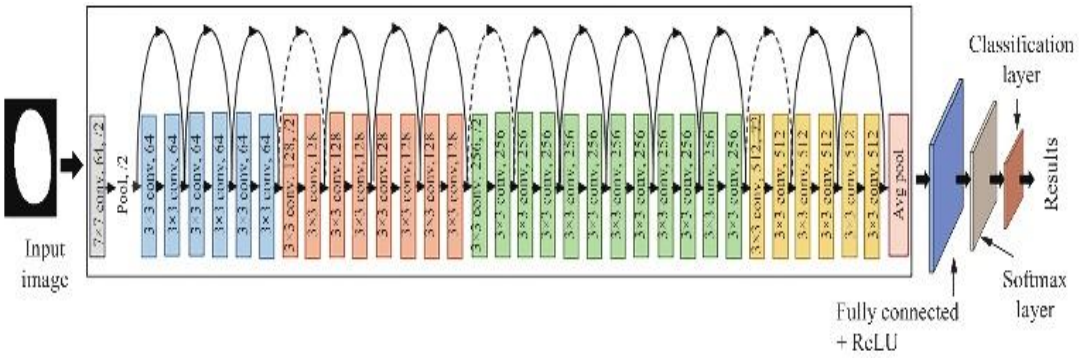

Figure 4. ResNet50 Architecture

3.4 Tools and techniques

This study was implemented using the Python programming language, selected for its robust ecosystem and extensive support for machine learning frameworks (Van Rossum & Drake, 2009). Model training and optimization were conducted within the Google Colab Pro environment, leveraging NVIDIA A100 Tensor Core GPUs to manage the high computational complexity inherent in deep learning tasks (Bisong, 2019). The neural network architectures were developed using TensorFlow and Keras (Abadi et al., 2016), which provided the necessary backend for the efficient deployment of the pre-trained ResNet50 and InceptionV3 models.

To ensure a rigorous assessment of model performance, a comprehensive suite of evaluation metrics was employed, including accuracy, precision, recall, and the F1-score. Furthermore, a confusion matrix analysis was conducted to provide a granular diagnostic of classification errors and to validate the models' discriminative power between myopic and emmetropic ocular states.

4. Results

4.1 Results of the ResNet50 model

Figure 5 presents the accuracy curves for both the training and validation phases of the ResNet50 architecture. These results demonstrate the model's ability to generalize effectively, showing a consistent upward trend in classification performance over the course of the training epochs.

Figure 5. Model accuracy curve during the training and validation phases

As illustrated in Figure 5, the ResNet50 model demonstrates rapid convergence, achieving accuracy values exceeding 99% within the initial training epochs. Following this early peak, the model maintains asymptotic stability with negligible fluctuations, reflecting a robust learning process. The close alignment between the training and validation trajectories indicates a high degree of generalization and an absence of significant overfitting. This consistency underscores the model's efficacy in extracting and utilizing discriminative features from the fundus imagery for precise myopia classification.

Complementing these results, Figure 6 depicts the progression of the loss function throughout the training phase. The downward trajectory of both training and validation loss further validates the optimization efficiency and the structural integrity of the model's learning architecture.

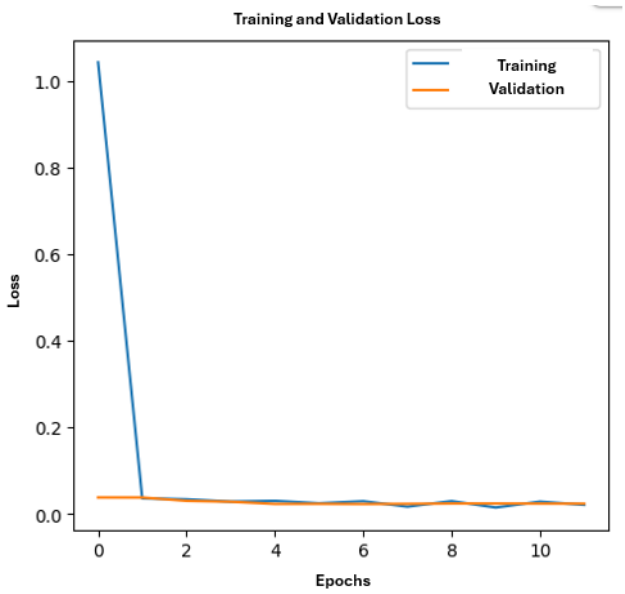

Figure 6. Model loss curves during training and validation.

As illustrated in Figure 6, the loss function exhibits a sharp initial decline, followed by steady convergence toward a terminal value of approximately 0.02. The minimal disparity between the training and validation loss curves confirms a stable optimization process and the absence of overfitting, thereby validating the model's convergence and robust learning behavior.

To further evaluate the model's discriminative performance on unseen data, a confusion matrix was generated using the independent test set, as presented in Figure 7. This matrix provides a granular visualization of the model's classification accuracy and its ability to minimize false positives and false negatives.

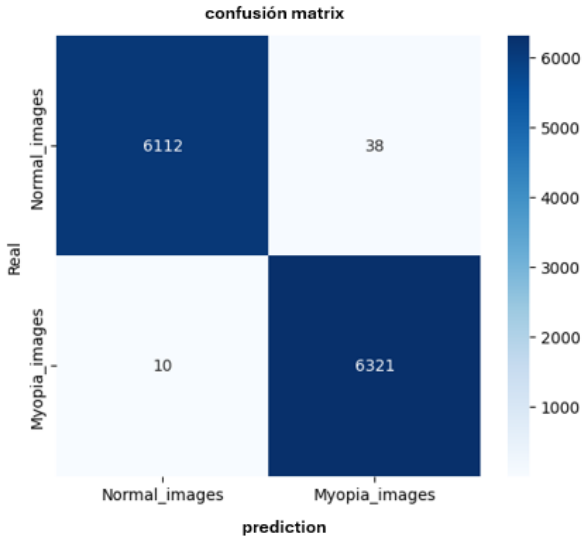

Figure 7. Model confusion matrix

Figure 7 illustrates the confusion matrix for the ResNet50 model, demonstrating exceptional predictive accuracy on the test set. Of the 12,481 total images analyzed, the model correctly identified 6,112 normal cases (True Negatives) and 6,321 myopic cases (True Positives). The model exhibited a remarkably low error profile, with only 38 false positives and 10 false negatives, resulting in an overall error rate of less than 0.4%.

From a clinical perspective, the minimal false-negative rate (0.08%) is particularly significant. In diagnostic support systems, prioritizing sensitivity is essential to ensure that myopic conditions are not overlooked, thereby facilitating timely medical intervention. These results underscore the model's reliability and its potential utility as a high-precision screening tool in clinical settings.

4.2 Results of the InceptionV3 Model

The temporal progression of the InceptionV3 model's accuracy during the training and validation phases is illustrated in Figure 8. This visualization tracks the model's performance over successive epochs, providing a clear representation of its learning curve and the stability of its high-precision classification on the fundus imagery dataset.

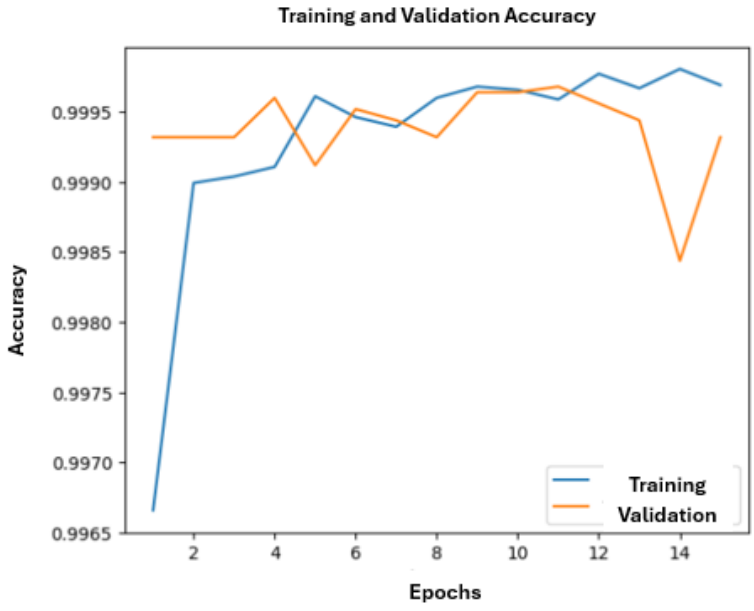

Figure 8. Precision curves for the model during training and validation.

As illustrated in Figure 8, the InceptionV3 model achieves accuracy levels exceeding 99.9% from the initial training epochs, maintaining exceptional stochastic stability throughout the entire optimization process. The near-perfect alignment between the training and validation trajectories reflects a remarkable generalization capacity, with no observable divergence to suggest overfitting. This performance pattern

underscores the efficacy of the InceptionV3 architecture in capturing complex hierarchical representations and subtle spatial patterns within the fundus imagery.

Furthermore, Figure 9 depicts the progression of the loss function during training. The rapid and consistent decline in loss values further validates the model's architectural efficiency and its superior ability to minimize error in the classification of myopia.

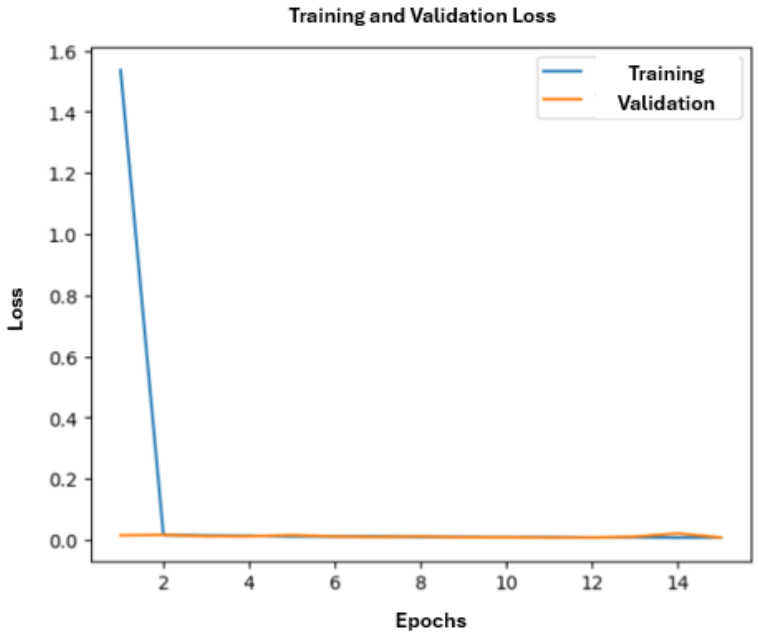

Figure 9. Model loss curves during training and validation

As shown in Figure 9, the loss function exhibits a precipitous decline during the first epoch, followed by steady convergence toward an asymptotic value of approximately 0.008. The stability of the optimization phase is further evidenced by the near-complete overlap between the training and validation trajectories. This behavior confirms that the model achieved an optimal fit while maintaining superior generalization capacity, effectively mitigating the risk of overfitting.

To provide a granular assessment of the model's diagnostic accuracy, the confusion matrix derived from the independent test set is presented in Figure 10. This visualization allows for a detailed examination of the model's discriminative performance across both myopic and emmetropic classifications.

Figure 10 presents the confusion matrix for the InceptionV3 architecture, revealing a superior predictive profile. Of the 12,481 total test images, the model correctly classified 6,141 normal cases and 6,329 myopic cases. The error distribution was remarkably minimal, consisting of only nine false positives and two false negatives, resulting in a cumulative error rate of less than 0.1%.

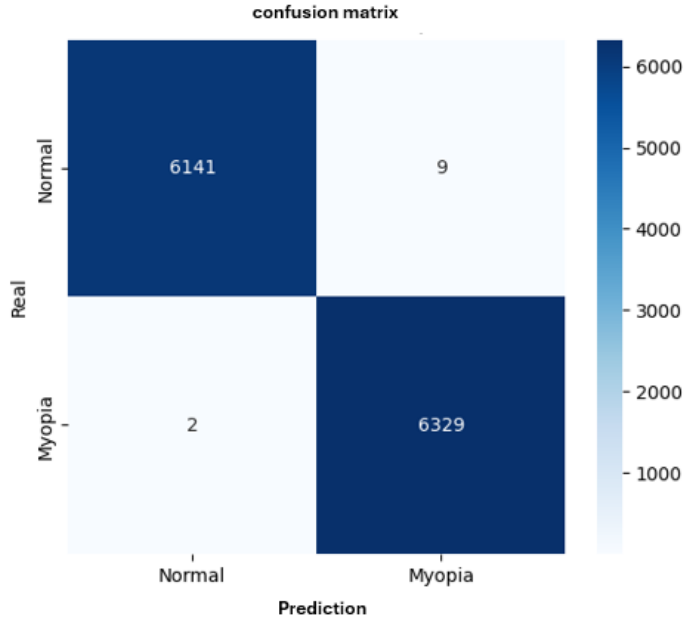

Figure 10. Confusion matrix for the model classifying normal and myopic images.

From a clinical standpoint, this near-zero false-negative rate is of paramount importance. In a screening context, the model's sensitivity (99.97%) virtually eliminates the risk of diagnostic oversight, ensuring that myopic patients are accurately identified for early intervention. These findings position the InceptionV3 architecture as an exceptionally reliable and robust tool for integration into automated ophthalmic diagnostic systems.

4.3 Model Comparison

Table 3 provides a comprehensive summary of the primary performance metrics achieved by both models on the standardized test set. This comparative overview facilitates a direct benchmarking of accuracy, precision, recall, and F1-score, highlighting the quantitative differences between the ResNet50 and InceptionV3 architectures.

Table 3: Performance Comparison Between ResNet50 and InceptionV3

Metric / Model	ResNet50	InceptionV3
Accuracy (Training)	99.67%	99.99%
Accuracy (Validation)	99.66%	99.97%
Loss	0.0232	0.0075
False positives	38	9
False negatives	10	2
Recall (Myopia)	1.00	1.00
Overall F1-score	1.00	1.00
Total errors	48	11

The comparative results in Table 3 demonstrate that the InceptionV3 architecture consistently outperforms ResNet50 across all critical performance indicators, including cumulative error count, categorical cross-entropy loss, and overall accuracy. Notably, InceptionV3 exhibits superior discriminative power, achieving a reduction in total misclassifications of over 77% compared to ResNet50 (11 vs. 48 errors). This substantial improvement in diagnostic precision, particularly at such high accuracy thresholds, underscores the robustness of the InceptionV3 framework for high-stakes clinical screening tasks.

5. Discussion

The findings of this study demonstrate that both InceptionV3 and ResNet50 architectures deliver exceptional performance in the automated classification of myopia via fundus imagery. Both networks achieved accuracy levels exceeding 99.6%, characterized by minimal loss values and high consistency between training and validation phases, which underscores their robust generalization capabilities.

The ResNet50 model exhibited rapid convergence and high stability, reaching a validation accuracy of 99.66% with a terminal loss of approximately 0.02. The alignment of the learning trajectories confirms that the architecture successfully extracted discriminative features without succumbing to overfitting. This was further validated by the confusion matrix, which recorded only 48 errors out of 12,481 test images. Notably, the low incidence of false negatives ($n=10$) is a critical metric, reinforcing the model's viability for clinical screening where diagnostic omissions must be minimized.

Conversely, the InceptionV3 model demonstrated superior optimization and even more remarkable performance metrics. Achieving a validation accuracy of 99.97% and a loss below 0.01, the architecture proved to be highly efficient in its learning process. The confusion matrix revealed a total of only 11 errors, significantly reducing both false-positive and false-negative rates compared to ResNet50. This superior performance is likely attributable to the Inception modules' capacity for multi-scale feature extraction, which allows for the detection of both global and local structural patterns within complex ophthalmic imagery.

In conclusion, while both architectures provide clinically reliable performance, the comparative analysis establishes InceptionV3 as the more robust and precise framework for diagnostic support systems. These results align with the existing literature that advocates for the efficacy of multi-scale CNNs in medical imaging. Furthermore, the findings confirm that these models maintain an ideal balance between sensitivity and specificity, positioning them as feasible, high-precision tools for real-world automated ocular diagnostics.

6. Conclusion

The experimental analysis confirms that both InceptionV3 and ResNet50 architectures provide highly efficient performance for the automated detection of

myopia in fundus imagery. Both models achieved precision, recall, and F1-score values approaching unity (1.0), demonstrating exceptional discriminative capacity. The comparative evaluation establishes InceptionV3 as the superior architecture, characterized by higher accuracy across all phases, significantly reduced loss, and a marked reduction in total classification errors relative to ResNet50. These results indicate a more effective optimization of the hierarchical learning process and greater structural robustness.

The convergence of the training and validation trajectories for both models underscores a high generalization capacity and the absence of overfitting, ensuring the reliability of the diagnostic output. Notably, the minimal incidence of false negatives—particularly within the InceptionV3 framework—is of paramount clinical significance, as it mitigates the risk of diagnostic oversight. This behavior reinforces the potential of these architectures as highly sensitive diagnostic support tools for the early identification of myopia.

Based on these findings, we recommend the prioritization of the InceptionV3 architecture for integration into automated screening systems and clinical diagnostic workflows due to its superior precision and lower error profile. Future work should focus on implementing k-fold cross-validation and testing against external, multi-center datasets to further validate these models in diverse, real-world clinical environments.

The proposed system architecture allows for the seamless upload of ophthalmic imagery, where clinicians can select between the InceptionV3 or ResNet50 models for automated analysis. The platform generates real-time predictions integrated with probabilistic confidence scores, facilitating a rapid and highly accurate visual assessment of myopia. This transparent output provides clinicians with quantifiable certainty levels, supporting more informed diagnostic decision-making.

7. References

Abadi, M., Barham, P., Chen, J., Chen, Z., Davis, A., Dean, J., Devin, M., Ghemawat, S., Irving, G., Isard, M., Kudlur, M., Levenberg, J., Monga, R., Moore, S., Murray, D. G., Steiner, B., Tucker, P., Vasudevan, V., Warden, P., … Xiao, Y. (2016, November 2–4). *TensorFlow: A system for large-scale machine learning* [Paper presentation]. 12th USENIX Symposium on Operating Systems Design and Implementation (OSDI 16), Savannah, GA, United States, 265–283. https://www.usenix.org/conference/osdi16/technical-sessions/presentation/abadi

Bisong, E. (2019). *Building machine learning and deep learning models on Google Cloud Platform: A comprehensive guide for beginners.* Apress. https://doi.org/10.1007/978-1-4842-4470-8

Cahya, F. N., Hardi, N., Riana, D. & Hadianti, S. (2021). Klasifikasi penyakit mata menggunakan convolutional neural network (CNN). *SISTEMASI, 10(3),* 618–626. https://doi.org/10.32520/stmsi.v10i3.1248

Celano, G. G. A. (2021). *A ResNet-50-Based Convolutional Neural Network Model for Language ID Identification from Speech Recordings* [Paper presentation]. Proceedings of the Third Workshop on Computational Typology and Multilingual NLP, Online, 107–111. https://aclanthology.org/2021.sigtyp-1.13

Fricke, T. R., Jong, M., Naidoo, K. S., Sankaridurg, P., Naduvilath, T. J., Ho, S. M., Wong, T. Y., & Resnikoff, S. (2018). Global prevalence of visual impairment associated with myopic macular degeneration and temporal trends from 2000 through 2050: Systematic review, meta-analysis and modelling. *British Journal of Ophthalmology, 102(7)*, 855–862. https://doi.org/10.1136/bjophthalmol-2017-311266

Hartati, E. (2024). Klasifikasi penyakit mata menggunakan convolutional neural network model Resnet-50. *Jurnal Rekayasa Sistem Informasi dan Teknologi, 1(3),* 199–206. https://doi.org/10.59407/jrsit.v1i3.529

He, K., Zhang, X., Ren, S., & Sun, J. (2016). *Deep residual learning for image recognition*. [Paper presentation]. Proceedings of the IEEE Conference on Computer Vision and Pattern Recognition, 770–778. https://openaccess.thecvf.com/content_cvpr_2016/html/He_Deep_Residual_Learning_CVPR_2016_paper.html

Holden, B. A., Fricke, T. R., Wilson, D. A., Jong, M., Naidoo, K. S., Sankaridurg, P., Wong, T. Y., Naduvilath, T. J., & Resnikoff, S. (2016). Global prevalence of myopia and high myopia and temporal trends from 2000 through 2050. *Ophthalmology, 123(5)*, 1036–1042. https://doi.org/10.1016/j.ophtha.2016.01.006

Jatmoko, D., & Lestiawan, H. (2024). *Prediksi penyakit mata menggunakan convolutional neural network*. [Paper presentation]. Proceedings Semnas Ristek (Seminar Nasional Riset dan Teknologi), 8(1), 851–857. https://doi.org/10.30998/semnasristek.v8i01.7129

Jonas, J. B., Bikbov, M. M., Wang, Y.-X., Jonas, R. A., & Panda-Jonas, S. (2023). Anatomic peculiarities associated with axial elongation of the myopic eye. *Journal of Clinical Medicine, 12(4),* 1317. https://doi.org/10.3390/jcm12041317

Kaya, M. (2025). Efficient diagnosis of retinal diseases using convolutional neural networks. *Gazi University Journal of Science Part A: Engineering and Innovation, 12(1),* 15–35. https://doi.org/10.54287/gujsa.1592915

Laksono, G. I., & Winarno, S. (2025). Myopia identification by fundus photo image classification using convolutional neural network. *Journal of Applied Informatics and Computing, 9(5),* 2801–2806. https://doi.org/10.30871/jaic.v9i5.10624

Primadiani, I. S., & Rahmi, F. L. (2017). Faktor-faktor yang mempengaruhi progresivitas miopia pada mahasiswa kedokteran. *Jurnal Kedokteran Diponegoro, 6(4)*, 1505-1517. https://ejournal3.undip.ac.id/index.php/medico/article/viewFile/18381/17461

Puspitasari, N., Utami, D., Sulistyawati, A., & Simanjutak, H. (2024). *Gambaran kelainan refraksi pada siswa/i di SDN Padaulun Kecamatan Majalaya tahun 2024*. Nama Orang.

Sait, W., & Rahaman, A. (2023). Artificial intelligence-driven eye disease classification model. *Applied Sciences, 13(20),* 11437. https://doi.org/10.3390/app132011437

Sambulele, A. P., Najoan, I. H. M., & Supit, W. P. (2025). Gambaran kejadian miopia pada mahasiswa Fakultas Kedokteran Universitas Sam Ratulangi. *Medical Scope Journal, 7(1),* 85–90. https://doi.org/10.35790/msj.v7i1.55450

Sanderson, K. (n.d.). Myopia image dataset. Kaggle. Retrieved December 23, 2025, from https://www.kaggle.com/datasets/kellysanderson/myopia-image-dataset

Shyamalee, T., & Meedeniya, D. (2022). CNN based fundus images classification for glaucoma identification. [Paper presentation]. 2022 2nd International Conference on Advanced Research in Computing (ICARC), 200–205. https://doi.org/10.1109/ICARC54489.2022.9754171

Simarmata, M. M., Doringin, F., Khofifah, N. A., & Aulia, Z. R. (2024). Upaya pencegahan miopia pada anak-anak sekolah dalam rangka Hari Kesehatan Nasional di Jakarta Convention Center. *Jurnal Peduli Kesehatan Mata*, 2(4), 48-57. https://doi.org/10.54363/pkm.v2i4.249

Singh, H., Singh, H., Latief, U., Tung, G. K., Shahtaghi, N. R., Sahajpal, N. S., Kaur, I., & Jain, S. K. (2022). Myopia, its prevalence, current therapeutic strategy and recent developments: A review. *Indian Journal of Ophthalmology, 70(8),* 2788. https://doi.org/10.4103/ijo.IJO_2415_21

Steinmetz, J. D., Bourne, R. R. A., Briant, P. S., Flaxman, S. R., Taylor, H. R. B., Jonas, J. B., Abdoli, A. A., Abrha, W. A., Abualhasan, A., Abu-Gharbieh, E. G., Adal, T. G., Afshin, A., Ahmadieh, H., Alemayehu, W., Alemzadeh, S. A. S., Alfaar, A. S., Alipour, V., Androudi, S., Arabloo, J., … Vos, T. (2021). Causes of blindness and vision impairment in 2020 and trends over 30 years, and prevalence of avoidable blindness in relation to VISION 2020: The Right to Sight: An analysis for the Global Burden of Disease Study. *The Lancet Global Health, 9(2),* e144–e160. https://doi.org/10.1016/S2214-109X(20)30489-7

Swain, S., & R, S. (2023). Prediction of myopia progression based on artificial intelligence model. In *Applied Mathematics, Modeling and Computer Simulation* (pp. 940–950). IOS Press. https://doi.org/10.3233/ATDE231034

Szegedy, C., Vanhoucke, V., Ioffe, S., Shlens, J., & Wojna, Z. (2016). Rethinking the inception architecture for computer vision. [Paper presentation]. Proceedings of the IEEE Conference on Computer Vision and Pattern Recognition, 2818–2826. http://doi.org/10.1109/CVPR.2016.308

United Nations. (n.d.). Sustainable Development Goals. https://www.un.org/sustainabledevelopment/

Van Rossum, G., & Drake, F. L. (2009). *Python 3 Reference Manual*. CreateSpace.

Wardhani, A. S., Anggraeny, F. T., & Rizki, A. M. (2024). Penerapan model hibrida CNN-KNN untuk klasifikasi penyakit mata. *Jurnal Mahasiswa Teknik Informatika - JATI*, 8(3), 3662–3667. https://doi.org/10.36040/jati.v8i3.9774

Zahra, R. P., Zaldi, Z., Laszuarni, L., & Sarirah, M. (2024). Risiko miopia terhadap jarak pandang dekat pada mahasiswa Fakultas Kedokteran Universitas Muhammadiyah Sumatera Utara. *Jurnal Pandu Husada, 5(4),* 8–21. https://doi.org/10.30596/jph.v5i4.21031.g12591

Zhang, H.-Q., Arif, M., Thafar, M. A., Albaradei, S., Cai, P., Zhang, Y., Tang, H., & Lin, H. (2025). PMPred-AE: A computational model for the detection and interpretation of pathological myopia based on artificial intelligence. *Frontiers in Medicine, 12*, 1529335. https://doi.org/10.3389/fmed.2025.1529335